

THERMO-MECHANICAL DAMAGE DUE TO LIGHTNING IMPACT IN CARBON/EPOXY COMPOSITES: EXPERIMENTS AND SIMULATIONS

Raúl Muñoz^a, Sofia Delgado^b, Federico Sket^a, Carlos González^{a,c,*}, Bernardo López-Romano^b
De-Yi Wang^a, Javier LLorca^{a,c}

^aIMDEA Materials Institute, C/Eric Kandel, 2, 28906 Getafe, Madrid, Spain

^bFundación para la Investigación, Desarrollo y Aplicación de Materiales Compuestos (FIDAMC),
Avenida Rita Levi-Montalcini 29, 28906 Getafe, Madrid, Spain

^cPolytechnic University of Madrid, Department of Material Science, E. T. S. de Ingenieros de
Caminos, Ciudad Universitaria, 28040 Madrid

*carlosdaniel.gonzalez@imdea.org

Keywords: Carbon fiber laminates, lightning impact, damage modeling, finite element method

Abstract

Carbon fiber-reinforced polymers, used in primary structures for aircraft due to an excellent strength-to-weight ratio when compared with conventional aluminium alloy counterparts, may nowadays be considered as mature structural materials. However, one of the main drawbacks of using such composites entails their poor electrical conductivity when compared with aluminium alloy competitors that leads to lightning strikes being considered a significant threat during the service life of the aircraft. This paper presents a set of lightning impact test carried out in a composite material manufactured by resin transfer moulding with a detailed inspection of the damage mechanisms caused. A model based on the finite element method is presented to account for the temperature distribution caused by Joule overheating around the arc attachment point. The results of the model are compared with the LST experiments in terms of damage extension.

1. Introduction

The introduction of composites in primary structures of modern aircraft presents particular problems with regard to the threat of a lightning strike. Lightning strikes every aircraft on average at least once a year. While metallic structures, such as traditional aluminium airframes, are highly conductive, carbon fiber-reinforced polymers (CFRPs) have much lower electrical conductivity due to the dielectric behavior of the polymer matrix. Most of the lightning current remains on the external structure of aircraft manufactured with highly conductive materials (such as metals) and quickly exits without leading to serious damage. The significantly large electrical current generated by a lightning strike is not, however, conducted away by composite structures and a lightning strike may lead to dramatic consequences due to material melting or burning at lightning attachment points. This is due to Joule effect heating, arcing and sparking at bonds, hinges and joints, mechanical damage by shock waves, and ignition of vapors within fuel tanks. Hence, a better understanding of lightning strike damage mechanisms on composite materials is mandatory [1].

2. Materials and experimental techniques

The CFRP laminates used in this study were manufactured by resin transfer moulding. To this end, a laminate made up of 10 layers of 2x2 twill carbon fabric (G0986 from Hexcel with 300g/m² of areal weight and 6K HT5131 carbon fiber yarns) with the same orientation [0]10 were injected by using the bi-component HexFlow RTM6-2 epoxy resin. The standard cure cycle involves the application of a temperature cycle of 180°C with an injection pressure of four bars for two hours. Several panels of ≈450x450x3mm³ were manufactured for the physical simulation of a lightning impact. A set of lightning strike tests (LSTs) were conducted by the Fundación para la Investigación, Desarrollo y Aplicación de Materiales Compuestos (FIDAMC) at the Laboratorio Central Oficial de Electrotecnia (LCOE) in Getafe, Madrid in accordance with the specifications included in the Aircraft Lightning Test Methods (EUROCAE ED-105, ED-84 and ED-91 [2,3,4]) which define the waveforms and lightning impact zones corresponding to each application. For instance, the pulse current waveform defined by the standard and which includes four components is depicted in Figure 1a. Components A and D correspond to the initial lightning strike and re-strike and involve high currents of 200kA and 100kA, respectively, which act during short periods (≤500μs) (Figures 1b and 1c). The peak intensity in components B and C is much lower, although they are maintained over a longer period. Components A and D are responsible for most of the damage in composite skins and were the objective of the simulation in this research work.

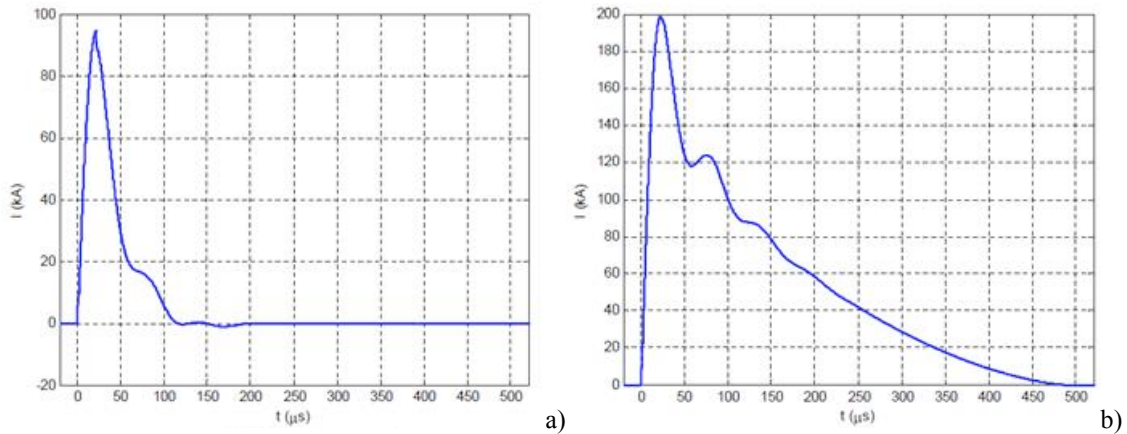


Figure 1. a) Level 1 waveform with maximum peak intensity of ≈100 kA, c) Level 2 waveform applied with maximum peak intensity of ≈200 kA.

The impulse current waveform, $i(t)$, can be described in terms of the total electrical charge Q and of the action integral I which measures the heat induced by Joule effect during the lightning impact. Mathematically, they are expressed by the following time integrals:

$$Q = \int_0^T i(t) dt \quad (1)$$

$$I = \int_0^T i^2(t) dt \quad (2)$$

where T is the total pulse duration. The square panels of 450x450mm² were placed in the testing rig and clamped on opposite sides. These sides were previously sanded to remove the

surface resin layer and improve electrical conductivity. The electrical current was injected at the centre of the panel. This was ensured by masking the outer surface of the panel with a dielectric material and exposing only a 150x150mm² square region at the centre, as well as connecting the panel to the cathode with a 100mm fuse wire to initiate the lightning arc. Before connecting the fuse wire, the surface panel was slightly chipped to facilitate the current transfer from the cathode to the composite panel. The panels were assembled in the laboratory test rig and connected to the waveform generator. Two tests, which corresponded to A and D current waveforms, were carried out on the panels.

3. Experimental results

The panels were visually and ultrasound inspected after the tests to ascertain the damage mechanisms caused by the simulated lightning impact. Ultrasound inspections were performed through use of the pulse-echo technique with water as coupling agent. The results of the inspections after impact revealed substantial fiber/matrix damage. Whereas surface recession was evident at the impacted face of all the panels, the rear face remained visually unaffected. Resin wear off at the lightning attachment point was mainly due to material pyrolysis caused by the high temperatures attained in this area, leaving naked and broken carbon fiber yarns at the panel surface, as Figure 2a) shows.

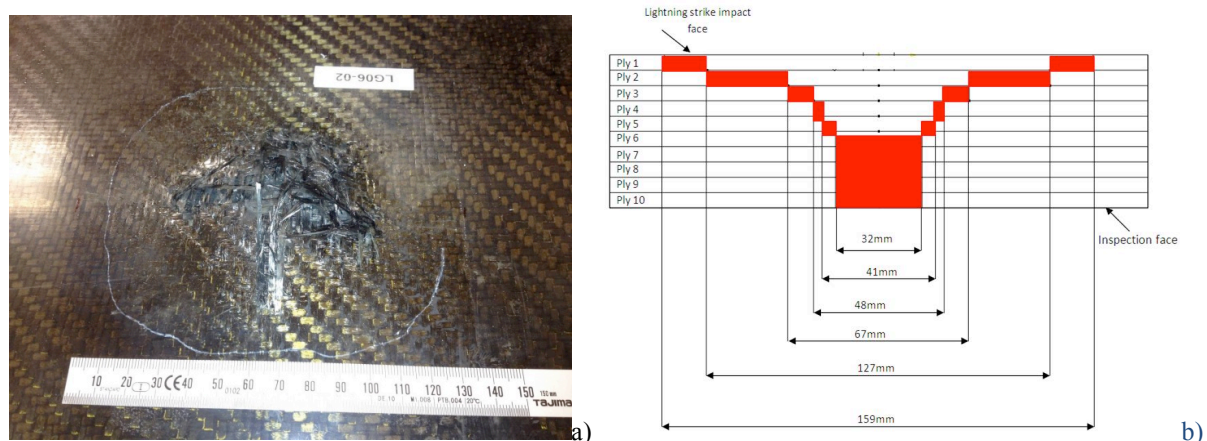


Figure 2. a) Detail of the damage around the lightning attachment point for A waveform impact. The rear zone of the panel remained visually unaffected, b)

The rapid expansion of material plasma around the attachment point creates strong shock waves that could lead to damage by spallation in the through-the-thickness direction. Damage by such spallation decreased with the distance to the attachment point of the lightning, even though evidence of resin thermal degradation (for example, open porosity) was observed in the region surrounded with a white line in Figure 2a). The circular shape of the damage zone is likely to be controlled by the isotropic in-plane thermo-electric properties of the twill fabric, as opposed to the behavior found in multiangular unidirectional composite laminates. Thermo-gravimetric analyses were performed using a thermo-balance (Q50 from TA Instruments) to examine the thermal degradation of the resin. The composite samples were heated at 10°C/min up to 500°C in N₂ and then in air from 500°C to 1000°C. The mass loss as a function of temperature showed that the thermal degradation of the resin took place in the temperature range between 200-600°C which can be used to estimate of the damaged area by temperature in the simulations. The damage penetration depth was also determined by means of ultrasound inspections, with the results obtained for the Level 1 in Figure 2b) in terms of penetration depth and average damage diameter. The inspections were performed from the

rear surface of the impacted panel. It should be mentioned that even if the rear face was visually unaffected, the ultrasound inspections revealed substantial attenuation when compared with the undamaged area which may be explained as being due to resin degradation caused by the thermal gradients or mechanical damage induced by electromagnetic and acoustic pressure.

The failure mechanisms were also studied by XCT using a Nanotom 160NF (Phoenix). The tomograms were collected at 100 kV and 210 μ A using a tungsten target. A Copper filter of 110 μ m was used to harden the X-rays. For the tomogram, 1800 radiographs were acquired with an exposure time of 1000 ms. The detector was moved perpendicular to X-rays to obtain a larger field of view (virtual detector, 2 tiles). Tomogram voxel size was set approximately to 29 μ m/voxel. The tomograms were then reconstructed using an algorithm based on the filtered back-projection procedure for Feldkamp cone beam geometry. Figure 3 shows the tomogram reconstructions where delamination are clearly observed in the first two-three layers of the laminate. However, the remaining material did not show significant macroscopic damage although the attenuation obtained by the c-scan signal indicated possible diffused damage.

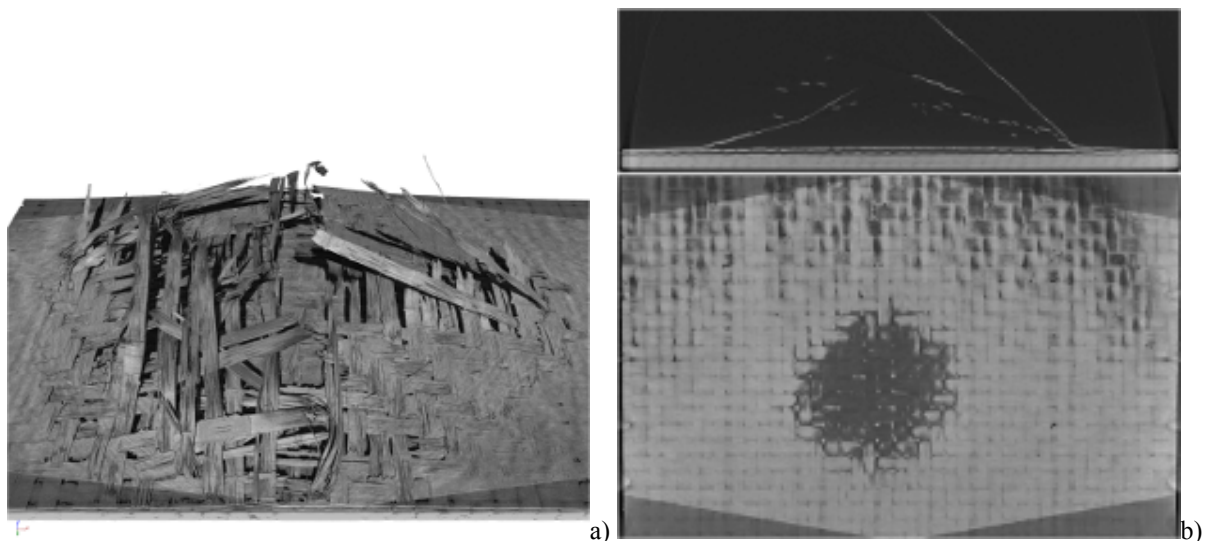


Figure 3. X-Ray tomography inspection of the impacted zone: a) Detail of the damage around the lightning attachment point for A waveform impact, b) Planar views showing extensive delamination in the first 2-3 layers of the composite laminate.

4. Model

A numerical model based on the finite element method was developed to address the effect of lightning impact on the carbon fiber-reinforced composite panels. A detailed analysis of this phenomenon will require the concurrent application of simulation strategies to address the complex multi-physics problem which accounts for the electromagnetic and acoustic pressures generated by the lightning current in combination with the Joule thermal effect. The heating of the composite panel due to the electrical resistance of the carbon composite was analyzed through using the coupled thermo-electric framework available in the Abaqus/Standard [5]. The models were run in an AMD Opteron cluster with 16 processors leading to \approx 4hours of computing time.

High-intensity currents flowing through a low-conductive material dissipate a large amount of heat by the Joule effect. The thermal degradation of the material leads to vapor generation that could trigger explosions, causing structural damage in composite skins. The panel behavior under this scenario can be obtained by a coupled thermo-electrical simulation. The electric field problem is governed by the charge conservation equation, which is expressed under the steady state current flow as,

$$\text{div}\mathbf{J} = r_c \quad (3)$$

where \mathbf{J} is the current density (current per unit area) and r_c the internal volumetric current source per unit volume. Ohm's law establishes the constitutive relation between the current density and the electrical field \mathbf{E} according to

$$\mathbf{J} = \boldsymbol{\sigma}\mathbf{E} \quad (4)$$

where $\boldsymbol{\sigma}$ is the electrical conductivity tensor. The electrical conductivity tensor was assumed to be anisotropic and controlled by the in-plane ($\sigma_{//}$) and through-the-thickness (σ_{\perp}) electrical conductivity of the composite. The in-plane conductivity is dictated by the continuous carbon fiber yarns architecture, while the out-of-plane behavior depends on the electrical behavior of the resin. The typical in-plane and out-of-plane electrical conductivity ratio of fiber-reinforced carbon composites is of the order of $\approx 10^3$ - 10^4 . The electrical conductivities were measured at EADS IW in France and the corresponding values were, respectively, $\sigma_{//}=14631\text{S/m}$ and $\sigma_{\perp}=2.7\text{S/m}$. In the absence of more specific data, the electrical conductivity was assumed to be temperature independent with the exception of the transversal value, which was five times higher for temperatures in excess of 600°C . This particular behavior was introduced to simulate the surface recession revealed in the experiments and has also been used by other authors [5,6]. The flow current front could be estimated by assuming this temperature dependence of the electrical conductivity. This heat generated by Joule effects is dissipated into the bulk by conduction through the composite material according to

$$\rho c_v \frac{\partial \theta}{\partial t} + \mathbf{k} \cdot \text{grad} \theta = q \quad (5)$$

where ρ is the material density, c_v the specific heat, \mathbf{k} the thermal conductivity tensor, θ the temperature, and q the volumetric heat generation (coming from the Joule electrical effect). The heat was set to $1065\text{J/Kg}^{-1}\text{K}^{-1}$, while the thermal conductivity was 5.9 and $0.69\text{Wm}^{-1}\text{K}^{-1}$ for the in-plane and through-the-thickness directions, respectively, assuming a cross-ply carbon fabric configuration [5, 6]. Additionally, thermal radiation was included in the model, which allowed heat exchange through the panel surfaces. Radiation effects using the Stefan-Boltzmann equation were also included in the model.

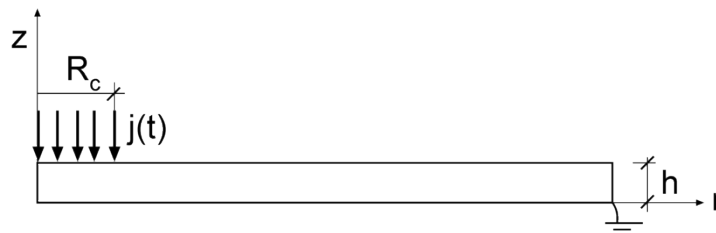


Figure 4. Cross section of the panel in the r - z plane indicating the domain of resolution of the thermal/electrical problem.

The coupled partial differential equations were solved by means of the finite element method by using Abaqus/Standard. The impacted panel was modeled by assuming axial symmetry (with r and z being, respectively, the radial and through-the-thickness directions) and, therefore, only the rectangular cross section of $225 \times 3 \text{ mm}^2$ in the r - z plane was discretized, Figure 4. This simplification of the real three-dimensional problem was carried out by taking into account the axial symmetry around the z axis of the damaged areas visualized with ultrasound inspections and allowed an accurate resolution of the thermal problem by using a detailed discretization with 50 elements in the through-the-thickness direction of the panel. This extremely fine mesh is required due to the large anisotropy in the electrical and thermal conductivity between the in-plane and the through-the-thickness directions which promoted flat thermal exposed areas with a lenticular shape. Typically, the model includes around 80000 DCAX4E elements in Abaqus Standard (four-node axisymmetric elements with electrical-thermal degrees of freedom).

The electrical current $j(t) = I(t) / \pi R_c^2$ was injected at the centre of panel surface in a circular area of radius $R_c = 10 \text{ mm}$ equivalent to the arc radius, as shown in Figure 4. Despite the unavailability of the exact arc radius for the specific LST performed, the injected current is introduced in the model to avoid convergence problems that arise when the current is injected in individual nodes. Moreover, the area affected by thermal degradation was considerably larger than the arc radius and should have negligible effects on the final damaged area.

The degrees of freedom of the electrical potential of the nodes belonging to the edges of the plate ($r = 225 \text{ mm}$) were set to zero to simulate the ground connection in the experimental rig. It should be noted that this approach neglects the transient effects caused by the intensity waveform. Abaqus internally computes the electrical field distribution and the potential by using steady-state assumptions, with the corresponding field variables (energy dissipated) being transferred to the heat module to compute the evolution of the temperature.

The model described in the previous section was electrically loaded according to the boundary conditions shown in 3.1 and by using the experimental electrical waveforms recorded for the Level 1 and Level 2 tests. The snapshots of the temperature distribution around the attachment point are plotted in Figures 5a and 5b, respectively, for these two conditions after $500 \mu\text{s}$. As expected, the shape of the affected zone was strongly governed by the anisotropic electrical/thermal behavior of the composite material which yielded a lenticular zone affected by the heat generated by the electrical discharge in the material.

Strong temperature gradients between the affected and unaffected zones were clearly visible. As the temperature profile drops down to room temperature in a small number of elements, the need of a highly fine mesh in the through-the-thickness direction was clearly justified. It should be mentioned that the present model offers a crude approximation of the heat/electrical exchange between the lightning impact and the carbon panel. The model does not include the effect of surface recession due to thermal degradation of the material. Resin wear off at the attachment point was observed in the experiments, exposing unbounded and broken carbon fiber yarns. As a consequence, the recession of impacted surface made it difficult to interpret the exact location of the injection point acting during the current injection. A possible way to mitigate such effects could be to introduce temperature dependence in the through-the-thickness electrical conductivity which was set to five times the room temperature value for temperatures above 600°C . This kind of numerical artifact facilitates penetration of the injected current in the through-the-thickness direction, simulating the effect of the surface recession.

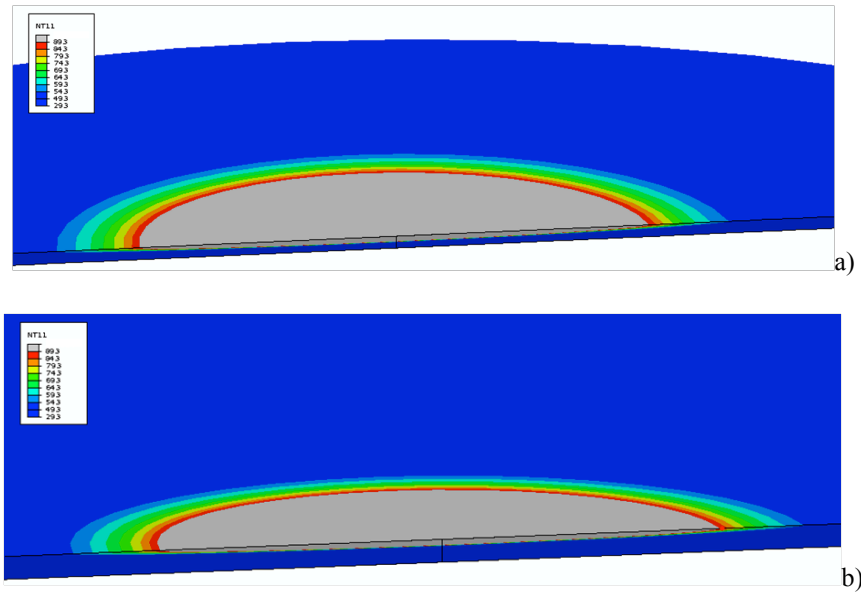


Figure 5: Contour plot of the temperature distribution immediately after application of the current waveform ($t \approx 500 \mu s$), a) Level 1 (Action integral $2.77 \times 10^6 \text{ A}^2 s$), b) Level 2 (Action integral $0.23 \times 10^6 \text{ A}^2 s$). Axisymmetric model sweep in the circumferential direction. Not scaled images.

Despite these unrealistic temperature values at the attachment points, the shape of the affected zone is reasonable and in good agreement with the experimental results. Following the work of Ogasawara [7], the zones affected by the heat were estimated from the temperature distribution obtained from the simulations. According to the thermo-gravimetric analysis performed on this material, the degradation of the resin took place in the temperature range of 200-600°C. This temperature range was selected as an objective criterion of thermal damage for quantification purposes from the contour plots obtained with the finite element model, Figure 8.

According to this criterion, surface extension of the damaged zone was reasonably captured by the model, Table 1.

LST Impact Type	Action Integral [$\text{A}^2 s$]	Damage Diameter Extension [mm]	Damage Depth [mm]
Level 1	2.77×10^6	125-177	1.32-1.53
Level 2	0.23×10^6	75-102	0.75-0.90

Table 1. Damage extension and penetration depth obtained in the FEM thermoelectric simulations. Lower and upper bound values of damage diameter and depth penetration were obtained assuming that the resin degradation occurs in the temperature range 200°C-600°C, respectively, according to TGA analysis.

However, the numerical simulations of the through-the-thickness damage penetration of 1.53 and 0.90mm for Level 1 and Level 2 impacts underestimated the experimental results obtained by ultrasounds, which showed significant attenuation signal below the attachment point, Figure 2b). The differences could be attributed to other sources of damage, such as the mechanical stresses produced by the electromagnetic and acoustic pressures. In this case, the acoustic and magnetic pressure gives rise to high bending stresses in the impacted area and damage by matrix cracking or delamination induced by these effects that could extend the damaged zone caused by Joule effects. In addition, such acoustic and electromagnetic actions also generate compressive through-the-thickness stress waves that rebound as tensile stresses at the rear face of the panel, leading to cracking and delamination by spallation.

5. Conclusions

Level 1 and Level 2 (≈ 200 and ≈ 100 kA of peak intensity) lightning impacts were performed in 3mm thickness carbon composite panels manufactured by RTM. The tests showed significant damage caused by lightning impact due to thermal degradation caused by Joule overheating. Surface recession by resin degradation was evident, leaving unbounded broken fiber yarns in the impacted face. X-ray tomography inspections revealed extensive damage by delamination occurred in the laminate. A coupled thermo/electric model was set-up to account for the Joule effects caused by the current transport through the material. The thermo-electric field equations were solved (including radiation effects) for the Level 1 and Level 2 electrical current waveforms. The results showed lenticular thermal affected areas, with a shape being determined by the mismatch in the in-plane and through-the-thickness thermal and electrical conductivities of the carbon composite material. The radius extension of the damaged zone was reasonably captured by the model by assuming that resin degrades in the 200-600°C range.

References

- [1] Modeling Lightning Impact Thermo-Mechanical Damage on Composite Materials, Raúl Muñoz, Sofía Delgado, Carlos González, Bernardo López-Romano, De-Yi Wang, Javier Llorca, Applied Composite Materials, 2014 (in press).
- [2] <http://www.eurocae.net/working-groups/wg-list/27-wg-31.html>. ED-105A Aircraft Lightning Test Method, ED-84A Aircraft Lightning Environment and Related Waveforms, ED-91 Aircraft Lightning Zoning Standard
- [3] SAE ARP 5412 and 5414. Aircraft Lightning Environment and related test waveforms.
- [4] SAE Technical Paper Series. Lynn L. Faulkner, Gene P. Shumaker. Prediction of aircraft structural damage from acoustic overpressures due to lightning strikes.
- [5] Abaqus/Standard/Explicit, Inc., Rising Sun Mills, Providence RI.
- [6] L. Chemartin, P. Lalande, B. Peyrou, A. Chazottes, P.Q. Elias, C. Delalondre, B.G. Cheron, F. Lago, Direct Effects of Lightning on Aircraft Structure: Analysis of the Thermal, Electrical and Mechanical Constraints, Journal of Aerospace Lab, 5, December 2012
- [7] Toshio Ogasawara, Yoshiyasu Hiran, Akinori Yoshimura, Coupled thermal–electrical analysis for carbon fiber/epoxy composites exposed to simulated lightning current, Composites Part A: Applied Science and Manufacturing, Volume 41, Issue 8, August 2010, Pages 973–981.